LIMNOLOGY
and
OCEANOGRAPHY

ASLO

Limnol. Oceanogr. 9999, 2020, 1–16

doi: 10.1002/lno.11467

Plant-mediated methane transport in emergent and floating-leaved species of a temperate freshwater mineral-soil wetland

Jorge A. Villa [1,2*] **Yang Ju,** [1] **Taylor Stephen,** [3] **Camilo Rey-Sanchez,** [1,4] **Kelly C. Wrighton,** [5] **Gil Bohrer** [1]

[1]Department of Civil, Environmental and Geodetic Engineering, The Ohio State University, Columbus, Ohio
[2]Now at School of Geosciences, University of Louisiana at Lafayette, Lafayette, Louisiana
[3]Department of Chemical, Biochemical and Environmental Engineering, University of Maryland – Baltimore County, Baltimore, Maryland
[4]Department of Environmental Science, Management and Policy, UC Berkeley, Berkeley, California
[5]Department of Soil and Crop Sciences, Colorado State University, Fort Collins, Colorado

Abstract

Methane flux from freshwater mineral-soil (FWMS) wetlands and its variability among sites is largely modulated by plant-mediated transport. However, plant-mediated transport processes are rarely resolved in land surface models and are poorly parametrized for plants commonly found in FWMS wetlands. Here, relationships between methane flux and CO_2 uptake, as well as plant conductance of methane were evaluated for three plant species and two characteristic functional types: emergent (narrow-leaved cattail) and floating-leaved (American lotus and water lily). We found significant but contrasting correlations between methane flux and CO_2 uptake in cattails (r^2 = 0.51, slope = –0.16, during morning) and water lily (r^2 = 0.32, slope = 0.064, after midday). This relationship was not significant in American lotus, showing that stomata regulation of methane fluxes is species-specific and not generalizable across the floating-leaved plant functional type. Conductance of methane per leaf area showed distinct seasonal dynamics across species. Conductance was similar among the floating-leaved species (6.2×10^{-3} m d^{-1} in lotus and 7.2×10^{-3} m d^{-1} in water lily) and higher than conductance in the emergent species (2.7×10^{-3} m d^{-1}). Our results provide direct observations of plant conductance rates and identify the vegetation parameters (leaf area, stomatal conductance) that modify them. Our results further suggest that models of methane emissions from FWMS should parameterize plant-mediated transport in different plant functional types, scaled by leaf area and with variable seasonal phenological dynamics, and consider possible species-specific mechanisms that control methane transport through plants.

It is estimated that ~ 30% of the methane emitted to the atmosphere is produced in wetlands, constituting the single largest natural source (Tian et al. 2016). Freshwater mineral-soil (FWMS) wetlands represent approximately 39% of the global area covered by wetlands, yet they account for up to 65% of the global methane emissions (Bridgham et al. 2006). In North America, it is estimated that FWMS wetlands account for up to 67% of wetland methane emissions (Kolka et al. 2018). However, estimates of methane emissions from these wetlands are still highly variable, in part, because of uncertainties in the rates of plant-mediated transport, which accounts for 30% to 90% of total methane fluxes (Van Der Nat and Middelburg 1998; Ding et al. 2002; Laanbroek 2010; Jeffrey et al. 2019).

*Correspondence: jorge.villa@louisiana.edu

Additional Supporting Information may be found in the online version of this article.

Methane is produced in wetland sediments and soils by methanogenic archaea after the stepwise degradation of organic matter under anoxic conditions (Segers 1998). Once produced, methane can be consumed by aerobic methanotrophic bacteria, or can be transported to the surface and emitted to the atmosphere via diffusion, ebullition, or plant-mediated transport. Methane transport through wetland plants is the result of an adaptative strategy of most macrophytes to transport oxygen from shoots to roots in order to thrive in the anoxic environment characteristic of wetland soils. Oxygen is transported as gas flows through an internal continuum of lacunar spaces formed by aerenchyma tissue connecting the rhizomes and the leaves (Colmer 2003). The flux in the lacunae is driven by gradients in pressure and humidity between internal gas spaces and the atmosphere (Dacey 1980, 1987; Beckett et al. 1988; Grosse et al. 1991; Tornberg et al. 1994). This mechanism, known as pressurized ventilation, occurs when oxygen-rich air from the shoots is vented down through the lacunae. Air with

high concentrations of methane, which diffused into the rhizome from soil pore water, is transported upward and eventually exits the plant through older leaves, damaged stems or leaves, stomata, or micropores in leaf sheaths (Nouchi et al. 1990; Armstrong and Armstrong 1991; Sorrell and Boon 1994). Molecular diffusion driven by concentration gradients inside the lacunae is another flux mechanism driving methane transport (Shannon et al. 1996), although this process is known to occur at a much lower rate and seems to predominate during the night when pressurized ventilation is suppressed (Chanton et al. 1993). Additionally, methane that is dissolved in pore water can be taken up by roots, transported by the sap through the xylem, and eventually transpired through stomata (Nisbet et al. 2009).

Previous observations have shown large variations in plant-mediated methane transport rates among species (Sebacher et al. 1983; Joabsson and Christensen 2001; Bhullar et al. 2013). Transport rates may scale with plant biomass (Kankaala et al. 2005; Kao-Kniffin et al. 2010), phenology (Koebsch et al. 2015), or age (Schütz et al. 1989). Depending on the specific design and regulation of the gas transport mechanisms in different wetland species, methane transport through the plant may be regulated by leaf photosynthesis and stomatal conductance, which are physiologically coupled as plants respond to light and CO_2 concentration and water vapor pressure gradients (Garnet et al. 2005; Matthews and Seymour 2014). Although the role of stomata regulation of methane fluxes has been observed in some plant species (Chanton et al. 1993; Morrissey et al. 1993; Thomas et al. 1996), the relationship between methane flux and carbon dioxide (CO_2) uptake and its variation among species have only be assessed in a few studies (Yavitt and Knapp 1995; Garnet et al. 2005).

Land-surface models that account for methane transport through plants as part of the prognostic process of surface methane flux in wet locations, typically assume a bulk plant-methane-transport conductance coefficient. There are very few observations with which to estimate such coefficients, and most of these are from northern peatlands, and not from FWMS nor from temperate wetlands and their associated plant species. Models diverge in their assumptions and consequent formulation of the type of regulation and dynamics of the plant conductance of methane. In most models, the end result of plant-mediated transport is simulated using a diffusive analogy, multiplying the soil-air concentrations gradient of methane (or some analog of that) by a bulk conductance, that is, the net conductance of the whole plant system to methane transport from the soil through the plant to the air, and not explicitly resolving within-plant processes such as pressurized ventilation transport or stomatal conductance (Xu et al. 2016). The methane transport conductance parameters for plants may be set to a constant value that represents the overall terrestrial and wetland biomes (Tian et al. 2010; Xu and Tian 2012). In some cases, models assume empirical values for conductance parameters that represent different plant functional types (PFTs; e.g., the Walter model, Walter and Heimann 2000 or Walter et al. 2001, and in the model ORCHIDEE, Ringeval et al. 2010). These values are based on the premise that physical traits in plants like root to shoot ratios and root distribution in the soil profile affect methane transport, but without a robust support from direct flux measurements. Alternatively, some models scale the conductance by leaf area, or stem area and stem porosity (CLM4Me, Riley et al. 2011; TRIPLEX-GHG, Zhu et al. 2014).

Aiming for a consistent representation of plant-mediated transport in FWMS wetlands and a better observation-based parametrization of plant transport in modeling efforts to constrain methane fluxes from wetlands ecosystems, we explored the flux rates and possible relationships between methane flux and CO_2 uptake rates in three common temperate FWMS wetland plant species of two different PFTs: emergent (cattail) and floating-leaved (American lotus and water lily). We predicted that if stomata regulate methane fluxes in any of the species, we would observe a positive correlation during the daytime between methane fluxes and CO_2 uptake. Furthermore, we predicted that bulk conductance of methane would be higher in floating-leaved than in the emergent species given their smaller root to shoot ratios and higher porosity.

Methods

Study site

The study was conducted in the Old Woman Creek (OWC), National Estuarine Research Reserve (NERR) in northern Ohio, at the coast of Lake Erie (41°22.758′N, 82°30.743′W, Fig. 1). The OWC is a drowned river-mouth wetland formed on Fluvaquents and Adrian muck soils (Natural Resources Conservation Service, 2017). OWC has a semipermanent connection with the lake that is constricted by the presence of a semiporous sand barrier that periodically forms at the wetland's mouth. As a result, a lagoon forms behind the barrier allowing the development of emergent and floating vegetation along the edges of the channel and in elevated deposits from autochthonous organic sources (Bernal and Mitsch 2012). Plant communities in OWC occur following the characteristic microtopographic zonation of most freshwater marshes (Mitsch et al. 2009). There is a zone at shallow and intermittent water levels (i.e., < 30 cm) dominated by emergent vegetation, and a zone with continuous standing water (i.e., > 30 cm) dominated by distinct patches of floating-leaved species. The deeper parts of the wetland along the river channel remain open water. The relative areal distributions of these plant communities show a clear interannual variability as a function of water levels (Whyte et al. 1997; Herdendorf et al. 2006).

Plant species description

Narrow-leaved cattail (*Typha angustifolia* L.), henceforth cattail, is an erect herbaceous plant with clonal growth, leaves as tall as 230 cm, rhizomes up to 70 cm deep (McNaughton 1966;

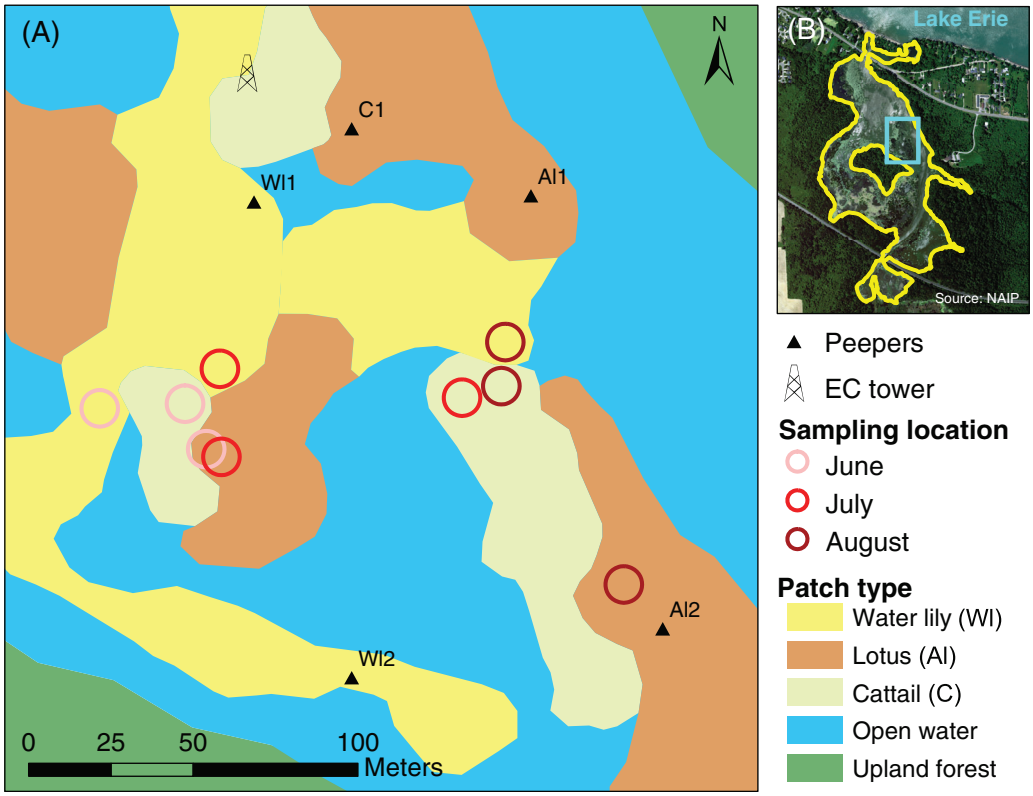

Fig. 1. Study site at the Old Woman Creek National Estuarine Research Reserve. **(A)** Location of monthly foliar methane flux and CO_2 uptake measurements, pore-water dialysis sampler (peeper) locations, and plant species distribution. **(B)** Relative location of the sampling area in the estuary (inner frame).

Grace and Harrison 1986), and root to shoot ratios typically 1 g g^{-1} d.wt under ambient nutrient levels (Li et al. 2010). Cattail has invasive traits and is common in restored and natural wetlands where it forms dense monostands often outcompeting other species (Fennessy et al. 1994; Tulbure et al. 2007; Cronk and Fennessy 2016). *Nelumbo lutea* (Willd.) Pers (American lotus) is an acaulescent herb, with orbicular flat floating leaves 30 to 60 cm in diameter that may emerge from the surface, and short adventitious roots extending from rhizomes that can grow deep in the soil up to 45 cm. *Nymphaeae odorata* Aiton (water lily) is an acaulescent herb as well, with orbicular floating leaves 10 to 30 cm in diameter and root to shoot ratios around 0.6 g g^{-1} d.wt (Richards et al. 2011). Both American lotus and water lily have a widespread distribution through North America (Schneider and Chaney 1981; McNaughton 1966), while cattail has a temperate and circumboreal cosmopolitan distribution. All three species are representative of cosmopolitan genera of macrophytes present in FWMS wetlands. The predominant gas transport mechanism in these species is pressurized ventilation, facilitated by the large and continuous lacunae spaces. In cattails, these spaces consist of a continuous aerenchyma tissue, while in American lotus and water lily of large air tube systems in the stems (Mevi-Schutz and Grosse 1988; Grosse et al. 1991; Chanton 2005).

Field sampling

Fluxes through plants

Methane flux and CO_2 uptake were determined simultaneously by cavity ring-down spectroscopy, using a portable greenhouse gas analyzer (Picarro G4301) coupled to custom-made leaf chambers (Fig. S1). Chambers consisted of transparent plastic storage boxes sealed with rimmed weather stripping and large binder clips. Chambers were fitted with a digital thermometer to monitor and record the temperature inside the chamber. Previous experiments with leaf chambers under sunny conditions indicated that, while net photosynthesis was not affected by the time of enclosure despite a significant increase in temperature, changes to methane fluxes and stomatal conductance could occur after 8 min of chamber deployment (Knapp and Yavitt 1992). To avoid such effects on stomatal conductance, we deployed our chambers for a conservative total measurement time of 4 min during which the chamber is closed. The Gas Scouter recirculated the air within the chamber while monitoring CO_2 and CH_4 concentrations simultaneously at a frequency of 1 Hz. The flow rate of chamber air through the Gas Scouter was ~1 L min^{-1}. The chamber used for sampling cattails had a volume of 3.364 L, and enclosed a section of few leaves, while the volume of the chamber used for American lotuses and water lilies was bigger

(12.437 L) allowing for the accommodation of an entire leaf without disruption. In addition, the chamber for floating-leaved species had two floating foams attached outside the chamber that kept it raised above the water level. Samplings were conducted monthly, from June through August 2018.

The sampling period encompassed the macrophyte peak growing season at OWC, aiming to exclude spring and fall transitions of vegetation growth and senescence that could bias the flux measurements. Sampling was conducted in the central portion of the estuary (Fig. 1). Every month, we randomly selected five adjacent leaves (floating-leaved species) or leaf sections (cattail) at different locations (Fig. 1). At each monthly sampling, chambers were deployed at three parts of the day: morning (08:00 h–11:00 h), midday (13:00 h–15:00 h), and afternoon (14:00 h–20:00 h). The morning time period included the peak in methane emissions (around 08:30 h), previously identified by Rey-Sanchez et al. (2018) in the sampling site. During each monthly campaign, we conducted the sampling of one species during a single day, except for June, when we sampled American lotus and water lily at the same day and cattail at the next day. Chambers were placed on the same leaves during the morning, midday and afternoon of the same day. These leaves were harvested at the end of the day. Chambers in cattails were placed 50 cm above the water surface, which was within the upper 2/3 of the leaves (Yavitt and Knapp 1995) and included five replicates of 4 to 6 leaf sections arrays at each enclosure. The sheath of the cattail leaves that we sampled was below the water level in all samplings. Measurements in American lotuses and water lilies were conducted on single floating leaves at five replicates. The leaves we sampled were already directly exposed to the atmosphere (i.e., not submerged). For gas flux measurements, the leaves were raised from the water surface and isolated in the chamber. After the sampling we checked for visible mechanical damage to the leaves that may have been caused during the daily sampling and thus compromised the sampling. We did not have to replace any measurement due to damage to leaves.

Leaf area

We measured the one-sided leaf area directly enclosed by the chamber by harvesting the leaves we sampled. We used one-sided leaf area because in the floating-leaf species methane flux to the air is done through the upper side of the leaf that is exposed to the air. Furthermore, one-sided leaf area is the standard vegetation property observed from remote sensing. To scale the flux from per leaf area in the chamber to flux per ground area for the plant type we also estimated the general leaf area index (LAI, m^2 m^{-2}) of each species after each diurnal sampling using a 0.25 m^2 PVC frame (five replicates) in the immediate area where we sampled. For American lotuses and water lilies, we took digital photographs that were processed to measure the proportion of area covered by leaves and then normalized by the area of the frame. We did not account for overlapping leaf areas as we assumed that submerged covered leaves do not participate actively in the exchange of gases with the atmosphere. Accordingly, the possible maximum LAI measured in floating-leaved species was 1. For cattails, we harvested the leaves inside the frame, clipping them at the water surface level, bagged and transported the leaves to the laboratory for further processing. Leaves from the June sampling were carefully measured to determine the area, then dried and weighted to generate an empirical allometric equation of specific leaf area to estimate LAI (unitless, m^2 leaf/m^2 ground) as a function of dry weight, W, (g) ($\mathrm{LAI} = 51\,W/A_f + 12.1$, $r^2 = 0.93$, $p < 0.001$, where A_f is the sample frame area, 0.25 m^2). We used this function to approximate the cattail LAI for July and August as a function of the dry weight of harvested biomass samples. We assumed that this allometric relationship between LAI and dry weight did not significantly change during the peak growing season (Weisner 1993).

Dissolved-gas pore-water concentrations

We measured methane pore-water concentrations at 10 depths from five in-situ dialysis samplers (peepers, MacDonald et al. 2013) deployed throughout the sampling area (Fig. 1). Each peeper consisted of 10, 61.4 mL, vertically spaced, inner cells. The distance between cells was 5.6 cm. Peeper cells were filled with DI water before deployment and after each sampling. Dissolved gases in the pore water diffused into the inner-cells through a polyethersulfon membrane with 0.22-μm pore size. Ten milliliters of subsamples from the cells were collected through a hosing system connected to each cell and placed in glass vials holding 0.2 mL of 1 M HCl to prevent microbial activity in the vial. Vials were filled to the top, crimped and kept refrigerated until processing (see MacDonald et al. 2013 for full details on sampler design, deployment, and operation). Once in the laboratory, concentrations of dissolved methane were obtained using the GC headspace equilibration technique (Kampbell et al. 1989). We used a 3-mL subsample from each vial to equilibrate in a 57-mL headspace of nitrogen.

The peepers represent a minimally disruptive way of sampling pore water and typically could be resampled on a frequency of once per 2 weeks or longer. Peepers were sampled within 2 d before the leaf-chamber samples. Unlike the gas concentration in the air, dissolved methane concentration in the pore water is changing slowly. Furthermore, the peepers equilibrate with the pore-water concentration through a dialysis filter membrane and take about 1 to 2 weeks to equilibrate fully. The peeper measurements, therefore, represent a slow ($\sim$ 10 d) moving average of the pore-water concentration of dissolved gasses during the same time that instantaneous leaf-level fluxes were measured.

Peepers in our site were installed 1 or 2 yr prior to this sampling campaign (Angle et al. 2017) and although the vegetation cover type changes between growing seasons, we did not move the peepers to minimize the disturbance to the sediments. We assumed that the mean pore-water concentration

observed in two peepers under a particular vegetation type was representative of this patch type throughout the central section of the wetland. The northernmost peeper, C1 (Fig. 1) currently located near the edge of a cattail patch, was originally placed near the center of a cattail-dominated area that started transitioning to American lotus in April to May 2018. When we sampled, the vegetation cover of this peeper comprised mostly dead cattail shoots and sparse lotus leaves. For our analyses, we assigned the observed pore-water concentrations from this peeper as characteristic to cattails. Because we could not reposition the peepers, we were limited in our ability to adjust pore-water sampling locations in response to changes in vegetation patch locations. We also do not know the vertical root-density distributions of the different plant species and therefore used a uniform vertical average of pore-water concentrations over the peepers' depth. Because of these limitations, the assumption that pore-water concentration in the peepers under each patch type is representative of the concentration experienced by each of that patch's plants is associated with large uncertainty. We address this uncertainty with an upper-bound uncertainty estimate using the vertical and lateral variation among all pore-water measurements (see more details of uncertainty estimates and their calculation approach in section 2.6 below).

Methane flux and conductance through plants

In each chamber measurement, we fitted the 4 min, 1 Hz time series of methane or CO_2 concentrations, C_{HM} (μmol mol^{-1}), to the nonlinear Hutchinson and Moiser one-dimension diffusion model (Hutchinson and Mosier 1981; Kutzbach et al. 2007; Pedersen et al. 2010):

$$C_{HM} = C_s + (C_0 - C_s)\, e^{-kt} \quad (1)$$

where C_0 is the predeployment concentration of methane or CO_2 (μmol mol^{-1}), C_s is the constant concentration component (μmol mol^{-1}), and k is a curve-shape parameter (s^{-1}). C_0, C_s, and k are determined by fitting the observed gas concentrations in the chamber C_{HM}, over time, t (s), using Eq. 1. We then calculated the flux, F, of methane and CO_2, F_{CH4}, and F_{CO2}, respectively (μmol m$_{leaf}^{-2}$ s^{-1}), at the leaf surface as:

$$F = k\,(C_0 - C_s)\,\frac{p\,V}{R\,Tch\,A} \quad (2)$$

where p (Pa) is the atmospheric pressure, measured at a nearby eddy covariance tower (Ameriflux site ID: US-OWC, Bohrer 2018); V the volume of the chamber (m^3), R the universal gas constant (8.314 m^3 Pa mol^{-1} K^{-1}), Tch the temperature inside the chamber (K), and A the area of the leaf enclosed in the chamber (m^2).

Examples for our flux calculation approach and quality control are provided in Fig. S2. Out of the 135 flux measurements, we discarded 31 where the goodness of fit for C_{HM} was lower than 0.9 ($r^2 < 0.9$) in either methane flux or CO_2 uptake. Discarded data were evenly distributed among species and did not show discernible patterns with the times of the day or month of sampling, except for measurements of cattails in June during morning time, which were all discarded (Table S1).

The apparent patch-level bulk plant conductance of methane from the soil to the atmosphere per leaf area, *CH$_4$conductance* (m d^{-1}), was calculated for each plant species as (after, Yavitt and Knapp 1995 and Nouchi et al. 1994):

$$CH_4conductance = \frac{F_{CH4}}{(C_{soil} - C_{air})}\,86400 \quad (3)$$

where C_{soil} (μmol m^{-3}) is the methane pore-water concentration at the day of sampling, calculated as the vertical average of the 10 peeper cells within the rooting zone (depths of 0–50 cm), in two peepers at the soil under each plant species (one for Cattail). C_{air} (μmol m^{-3}) is the equivalent aqueous concentration of methane in the air, and 86,400 is the number of seconds in 1 d.

We calculated C_{air} as:

$$C_{air} = C_{ch}\,pH^{cp} \quad (4)$$

where C_{ch} (μmol mol^{-1}) is the average five initial methane concentration measurements in each chamber deployment, p (Pa) is the atmospheric pressure and H^{cp} the Henry's solubility constant for methane (1.4×10^{-5} mol m^{-3} Pa^{-1}).

We estimated plant conductance of methane per ground area by multiplying *CH$_4$conductance* by the species-specific LAI. All data for and results of the conductance calculation are presented in Tables S1 and S3. The conductance we measure is the instantaneous conductance, averaged during 4 min of the chamber measurements. While it does not represent a daylong measurement, we chose to report it in m d^{-1} to keep consistency with the units reported in the literature and explicitly used in some land surface models (e.g., DLEM).

It is also important to note that this apparent patch-level bulk conductance is not exactly and exclusively the conductance of a particular plant tissue (root, stem, and leaf) to the movement of dissolved or gas-phase methane. Instead, it represents an assumed effective bulk conductance for movement of methane between the soil and the air although a pathway that typifies the vegetation within a certain ecosystem patch. In other words, it is the bulk conductance that models that do not explicitly resolve methane movement within the plants use to parameterize the plant flow contribution. We, therefore, do not calculate conductance values for individual plants but combine the patch-level mean plant-flow-through flux, the mean pore-water concentration over an assumed and equally distributed rooting depth, and the mean leaf area to calculate the apparent bulk conductance. We scale the conductance by leaf area as it is the most easily measurable

characteristic of any vegetated patch. We choose not to scale conductance by the stem or xylem diameter, or by vegetation height as these are typically unknown for particular patches at high (weekly) temporal resolution. Furthermore, the conductance we report represents the conductance of methane that is flowing through leaf blades exposed to the atmosphere, not accounting for methane that is diffused through the water column, even though some methane may enter the water column through the submerged parts of the plants. In this experiment, we particularly focused on flux from the plants to the air, and not of diffusive flux from the water column, as the latter is more commonly measured and reported for wetlands using floating chambers and modeled using a different parallel pathway of emission.

Relations between methane and carbon fluxes

To test whether methane flux is regulated by stomatal conductance, we measured the significance of a linear regression between methane flux and CO_2 flux (CO_2 uptake rate is driven by stomatal conductance) for each species. We hypothesize that if stomata control methane flux, the observed rate of methane flux in a chamber should be positively correlated with the rate of carbon uptake in the same chamber, as carbon uptake is, to a large degree and particularly during the day, controlled by stomata conductance. The regressions were performed pooling data across samples for the morning observations, midday and afternoon observations, and the overall combined diurnal sampling period. This grouping of the observations is driven by the assumption that methane accumulation at night when stomata are closed may flush out when stomata open in the morning and thus stomata–methane flux relationships in the morning may present different patterns than during the rest of the day.

Uncertainty analysis for conductance of methane through plants

We made two major assumptions in our patch-level bulk conductance calculations with regard to the concentration gradients (the denominator of the conductance calculation, Eq. 3). One is that the effective concentration controlling the diffusion of methane from the sediments to the roots system is uniform throughout the vertical extent of the top 50 cm of the sediment profile. This assumption is equivalent to assuming the rooting-depth distribution is uniform at depths between 0 and 50 cm. The other assumption we made is that vertically averaged pore-water concentrations are spatially homogeneous within each vegetation type and represented by the small sample of peepers in that patch. We estimated the maximal uncertainty associated with the vertical heterogeneity of pore-water concentrations by recalculating the conductance using the lowest and highest pore-water concentrations along the sediment profile at each vegetation type and sampling. We estimated the maximal uncertainty associated with the spatial heterogeneity of methane pore-water concentration by recalculating methane conductance using the lowest and highest vertically averaged pore-water concentrations at any given location in the entire site. For both uncertainty estimates, we used the range between the highest and lowest observed concentrations, rather than the standard deviation of the observations, to provide upper bounds to the uncertainty estimates.

Data analysis and availability

We processed data and conducted regression tests and fit models using MATLAB® 2018b. We used JMP 14® Pro 14.0.0 for all other statistical tests. All the statistical tests were conducted at a 0.05 significance level. We used Wilcoxon paired comparisons to test the differences between methane fluxes during different times of the day. To test the hypothesis of different conductance of methane in PFTs, we used an ordinal logistic model with conductance as the response variable, plant species as a fixed effect, and month of sampling nested by plant species. We used the same model setup to test for differences in CO_2 uptake at the leaf level for the plant species during the three monthly samplings.

Meteorological data for the measurement site at OWC are available through the National Estuarine Research Centralized Data Management Office (http://cdmo.baruch.sc.edu/get/landing.cfm), and through the Ameriflux site US-OWC (Bohrer 2018, https://ameriflux.lbl.gov/sites/siteinfo/US-OWC). Surface chamber measurements and pore-water concentrations for OWC, including these used in this study are available through The Department of Energy data portal – ESS-DiVE (Bohrer et al. 2019, https://data.ess-dive.lbl.gov/view/doi:10.15485/1568865).

Results and discussion

Species-specific mechanisms of plant methane-transport regulation

Median (and interquartile range) foliar methane fluxes for cattail (0.13 [0.032–0.61] μmol m_{leaf}^{-2} s^{-1}) were within the range reported for cattails in several wetlands of different climates in the USA (0.01–1.49 μmol m_{leaf}^{-2} s^{-1}, mean 0.22 μmol m_{leaf}^{-2} s^{-1}, Yavitt and Knapp 1995). Similarly, foliar fluxes from American lotus (0.34 [0.085–0.58] μmol m_{leaf}^{-2} s^{-1}) and water lily (0.47 [0.079–0.8] μmol m_{leaf}^{-2} s^{-1}) agree well with fluxes reported in other studies (0.2–1.8 μmol m_{leaf}^{-2} s^{-1}) for wetland plants common in FWS wetlands with pressurized ventilation and diffusion-driven flow (Garnet et al. 2005). We did not find statistical differences among the fluxes during different times of the day for any of the plant species (Fig. 2B,D,F), whereas observations in cattail were more variable in the morning and showed distinct higher observations extremes in the mid-to-late morning (Fig. 2A). Diurnal dynamics in plant methane flux were previously attributed to the gas transport mechanism (Chanton et al. 1993) and the regulating role of photosynthesis and stomatal conductance in gas exchange (White and Ganf 2000; Garnet et al. 2005; Matthews and

Seymour 2014), which are in turn dependent of variations in temperature and irradiance (Knapp and Yavitt 1995; Whiting and Chanton 1996). Garnet et al. (2005) estimated that stomatal conductance and net CO_2 assimilation accounted for up to half of the variation in methane flux among four wetland species of different life traits, although the effect of stomatal conductance was three times that of equivalent changes in CO_2 assimilation. Ruling out the effect of different transport mechanisms, they attributed the remaining variability to temperature, plant physical differences, such as the root surface area involved in methane uptake, and slow processes that operate at time scales exceeding the hourly scales, such as rhizosphere oxidation of methane or root carbon exudation.

We found negative correlations between methane flux and carbon uptake rates in cattails during the morning, and positive correlations between methane flux and carbon uptake rates in water lily during the afternoon and overall (Fig. 3). While correlation does not infer causation, strong mechanistic regulation of methane flux by stomata will lead to an apparent positive correlation between methane flux and carbon uptake, as they will both share a common regulatory mechanism. However, such a positive correlation could be misleading if methane and carbon flux are both correlated to other environmental drivers, for example temperature, soil moisture, or light. Yet, during the growing season, daytime temperatures do not limit photosynthesis and, thus, are not strongly

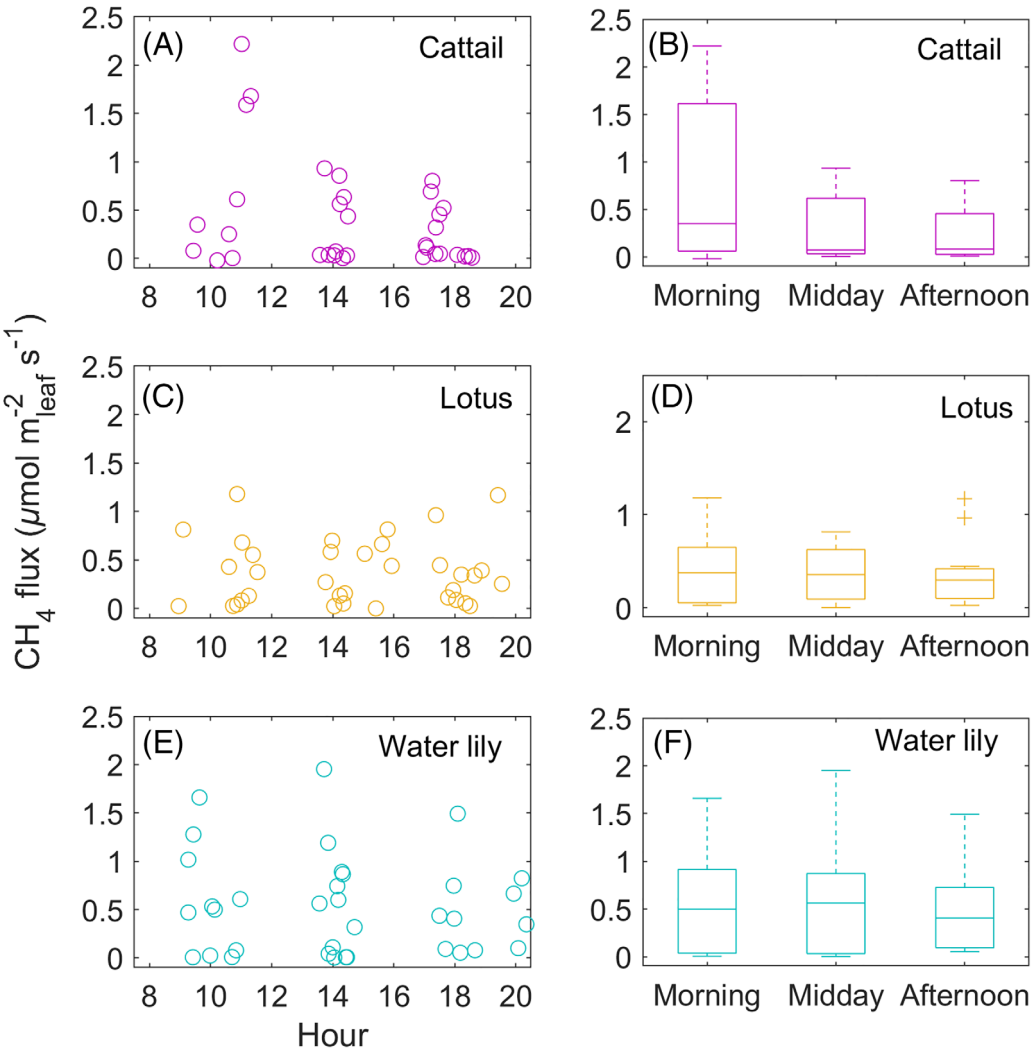

Fig. 2. Diurnal variation of methane fluxes through cattail **(A,B)**, American lotus **(C,D)**, and water lily **(E,F)**. Panels A, C, and E show the measurements at the moment of sampling per species. Panels B, D, and F show fluxes per species binned into diel periods: morning (08:00 h–11:00 h), midday (13:00 h–15:00 h), and afternoon (14:00 h–20:00 h). Horizontal lines represent median values, while tops, and bottoms of each box the interquartile range. Outliers, marked +, represent observations that are more than 1.5 times the interquartile range. Whiskers extend to the furthest observation not considered an outlier. Median flux at different times of the day was not statistically different for any species (Kruskal–Wallis test). Data comprise three monthly samplings conducted from June through August 2018.

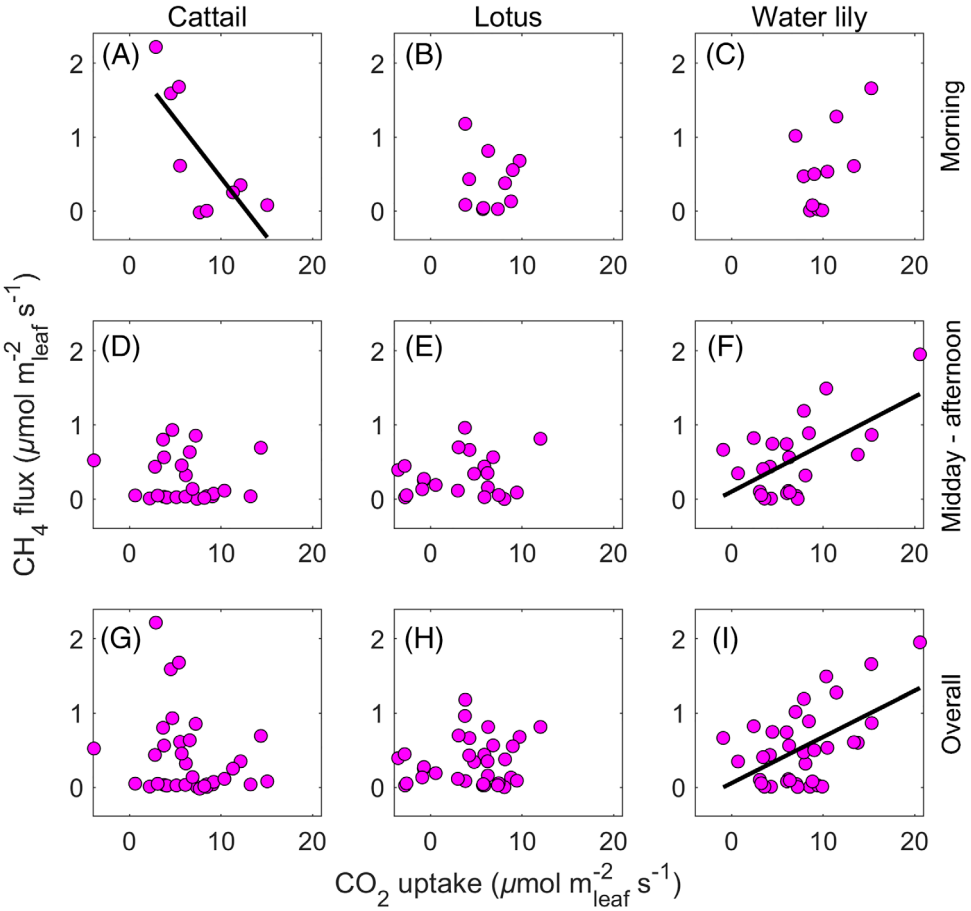

Fig. 3. Correlations between methane flux and CO_2 uptake for cattail **(A,D,G)**, American lotus **(B,E,H)**, and water lily **(C,F,I)**. Plots indicate significant correlations for cattail at morning (r^2 = 0.51, slope = −0.16, p = 0.018), and water lily at midday and afternoon (r^2 = 0.32, slope = 0.064, p = 0.002), and the overall sampling (r^2 = 0.26, slope = 0.063, p < 0.001).

correlated with daytime carbon uptake rate (Labate and Leegood 1988). Furthermore, wetland soil is essentially always flooded and thus photosynthesis in the wetland does not decrease due to water shortage (Farquhar and Sharkey 1982). Finally, photosynthesis and carbon uptake are controlled by light level, but light level is not expected to directly affect methane flux. Therefore, varying light levels during the daily measurements' times could add noise and obscure a stomata-driven correlation between carbon and methane fluxes, but light-level variations cannot generate a spurious positive correlation.

In cattail species, Yavitt and Knapp (1995) proposed that during the night when stomata are closed, and pressurized ventilation is negligible, soil-to-plant methane concentration gradients drive the diffusion of methane into the rhizome and from there to lower parts of the leaf. At sunrise, stomata open and pressurized ventilation are driven by temperature and humidity gradients between leaves and air resumes, fluxing out the methane, which has been accumulating during the night. Typically, methane fluxes exhibit a large transient peak at mid-to-late morning (Rey-Sanchez et al. 2019), associated with increasing light levels (Whiting and Chanton 1996). Later throughout the day, as methane concentration in the leaves decrease, methane fluxes become limited by pressurized ventilation and not by stomata conductance. Whiting and Chanton (1996) reasoned that the apparent control of stomata during the morning must be circumstantial after observing that the morning peak of methane flux occurred before the peak in stomatal conductance, which occurred later at mid-day. They argued that the initial opening of stomata allowed the release of methane explaining the peak in the morning, when light levels, and therefore CO_2 uptake rates, are low. Instead of functioning as a flux regulator, stomata function as a "release valve" for methane upon the initial opening. Our results indeed show a significant negative correlation between methane flux through cattail and CO_2 uptake during the morning, but not throughout the rest of the day (Fig. 3A,D,G), agreeing with this release valve hypothesis.

The flux of methane and its possible relationship with CO_2 uptake in floating-leaved species is less understood than it is

for cattails. We found a significant correlation between methane flux and CO_2 uptake in water lily (Fig. 3I). When breaking the measurements by the time of the day, the correlation was only observed after midday (Fig. 3F), when photosynthetic yields are at its maximum (Ritchie 2012), which strongly supports the assumption that methane is regulated by stomatal conductance in this species. However, a definite confirmation of a mechanistic link would require actual simultaneous measurements of stomatal conductance (Garnet et al. 2005). Interestingly, we did not find any correlation between methane flux and CO_2 uptake for the American lotus (Fig. 3B,E,H). Unlike other macrophytes, the flow of gases in lotus is actively regulated by large stomata found in the center of the leaves. These stomata, different from those found in leaf blades, open in the morning, close at midday, and reopen late in the afternoon, decreasing conductance in response to increasing light (Matthews and Seymour 2014). Possibly, the large central stomata do not account for the bulk of photosynthesis (Dacey 1987). This would decouple the CO_2 uptake observations from the conductance of these stomata that control methane flux, and lead to the apparent lack of correlation between methane flux and carbon uptake.

Overall, the data indicate that the relationship between methane flux and CO_2 uptake is different between the floating-leaved and emergent species. We found a contrasting correlation between cattail and water lily, and at different times of the day. However, our observations failed to show similarity in the methane–carbon flux relationship among the two floating-leaved species, showing that stomata regulation of methane fluxes is not necessarily generalizable to FWMS wetland species according to their growth-form characterization of PFT.

Conductance of methane is different among emergent and floating-leaved species

As expected, median (and interquartile range) methane conductance during the 3-month study period was similar in the floating-leaved species ($p = 0.27$), 6.2×10^{-3} (1.8×10^{-3} – 1.1×10^{-2}) m d^{-1} and 7.2×10^{-3} (1.2×10^{-3} – 1.6×10^{-2}) m d^{-1}, in lotus and water lily, respectively, and these significantly differed from that of the cattail ($p = 0.003$), an emergent species, 2.7×10^{-3} m d^{-1} (6.2×10^{-4} – 9.8×10^{-3}) (Fig. 4A). On top of the observed variability in methane conductance throughout the study period, we found high uncertainty due to vertical heterogeneity of methane pore-water concentrations. Our estimates indicate that uncertainty may account for up to 40% to 67% lower and 137% to 284% higher conductance (depending on species) than the median conductance values that we reported. This uncertainty due to the vertical concentration variations was considerably higher than the uncertainty due to the spatial heterogeneity of the mean profile concentrations (estimated to account for between 8%–34% lower and 11%–93% higher, depending on species; Table S2). Overall, the uncertainty associated with vertical and spatial heterogeneity of methane concentration in the soil is within the range of the observed variability of conductance. Therefore, we believe that such uncertainty does not obscure the actual values that our observations represent.

In general, our observations of conductance are low, and at, or somewhat below, the low end of the range reported by other studies based on partial field measurements or estimated from modeling approaches. For instance, DLEM, one of the available models capable of simulating plant-mediated methane transport uses a default conductance value of 0.68 m d^{-1}, selected as a median value from a range of 8×10^{-3} to 17.2 m d^{-1} reported in the literature (Tian et al. 2010; Xu et al. 2015). That median value is much higher than the average median value we observed for the two floating-leaved species (6.7×10^{-3} m d^{-1}) and the median value we observed for the cattail (2.7×10^{-3} m d^{-1}). Nonetheless, the values we observed are near the lower edge of the previously reported range. Our values were also an order of magnitude lower than the estimates for rice (3.5×10^{-2} m d^{-1}, Nouchi et al. 1994) and considerably lower than previously assumed conductance for cattail (1.78 m d^{-1}, Yavitt and Knapp 1995). The differences between our measurements and values measured in rice and assumed/observed in peatland PFTs may be due to the high porosity of peat soils that reduce the resistance of transport from soil to root (in the case of peatlands), or due to anatomical differences between plants species, such as xylem porosity or root to shoot length ratios (Smirnoff and Crawford 1983; Tornberg et al. 1994; Lorenzen et al. 2001; Richards et al. 2011).

The different plant species had distinct seasonal dynamics (Fig. 4A). In cattails, the median (and interquartile range) conductance per leaf area increase as the season progressed, from 3.8×10^{-4} (1.5×10^{-4}–5.1×10^{-4}) m d^{-1} in June to 7.6×10^{-3} (1.6×10^{-3}–1.2×10^{-2}) m d^{-1} in August. In contrast, conductance decreased in lotus from 9.6×10^{-3} (6.5×10^{-3} m d^{-1}–1.2×10^{-2}) m d^{-1} to 2.6×10^{-3} (9.3×10^{-4}–8×10^{-3}), while in lily peaked and was more variable in July 1.91×10^{-3} (7×10^{-3} – 3.2×10^{-2}) m d^{-1}. Seasonal variations in methane conductance through cattails could be associated with the controlling role of biomass in the pressurized ventilation. Convective throughflow in cattails is thought to initiate at the top parts of the leaves, where atmospheric humidity is relatively low, whereas internal air with methane is vented from lower parts of the leaves or older leaves in the culm (Yavitt and Knapp 1998). As the leaves grow taller, their potential for pressurized ventilation increases. Rising heights could explain our observations of more significant methane fluxes towards the middle and end of summer when the plants were taller, and thus their LAI was larger (Fig. 4B). Alternatively, the increase in conductance may be related to overall plant aging and the occurrence of senesced areas with larger pores that enhance flux by increasing conductance (Sebacher et al. 1985; Schütz et al. 1989; Constable et al. 1992). Seasonal peaks as observed in water lily may be explained, at least in part, by the direct link between methane flux and photosynthesis (Fig. 3I). Water lilies have relatively high photosynthetic

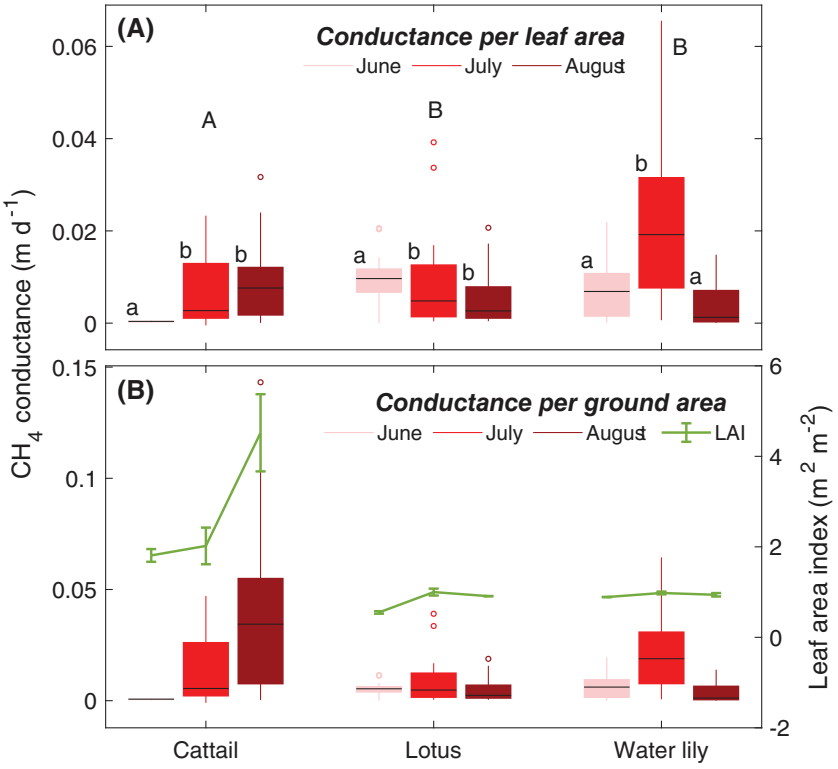

Fig. 4. Box plots of methane plant conductance for three common species of FWMS wetlands sampled monthly from June through August 2018. Horizontal lines represent median values, while tops and bottoms of each box the interquartile range. Outliers, shown as circles, represent observations that are more than 1.5 times the interquartile range. Whiskers extend to furthest observation not considered an outlier. **(A)** Shows methane conductance per leaf area error bars represent the convolution of variation in flux measurements and pore-water concentrations across different depths (0–50 cm) and locations in soil of the same vegetation patch. **(B)** Shows methane conductance per ground area (i.e., conductance in A × LAI). Error bars incorporate the variation of conductance per leaf area with the variation of leaf area measurements among five sample plots at the same time and vegetation type. Line plots in (A) represent mean (± SEM) LAI (right axis). Capital letters indicate differences at the species level while lower case letters the difference between samplings for each species. Conductance is significantly different between the emergent and floating-leaved species.

yields (Ritchie 2012), and the total photosynthetically active radiation during midday in the days we sampled water lilies peaked during July and drastically declined by the sampling in August due to cloud cover (Fig. S3).

When stomata are open, the limiting step in plant methane conductance is the diffusion of methane from the soil to the rhizomes (Beckett et al. 2001; Ding et al. 2004; Henneberg et al. 2012). Remarkably, we did not find a significant difference between species or during the season within species in per-leaf-area CO_2 fluxes (Fig. 5B). However, although we found variations in methane pore-water concentrations throughout the sampling period, none of the seasonal dynamics in plant flow-through fluxes followed the seasonal pattern of pore-water variation (Fig. 5A; Table S3). It is possible that the high concentrations in pore water in our site have supported constant high concentrations of methane in the lacunae, despite the seasonal variations. The pore-water concentrations we found at OWC are 3 to 20 times higher than the commonly reported in other wetland ecosystems (Chasar et al. 2000; Elberling et al. 2011; Wang et al. 2018). If variations in pore-water methane concentrations were not driving seasonal methane plant flow-through fluxes, then morphological and physiological differences in conductance among plant species must account for the seasonal-scale variability we observed in methane fluxes.

Conclusions and implications for modeling

Poor representation of plant conductance in process-based methane models is an important source of variability in model outputs (Tang et al. 2010). Our results offer valuable insights that could help improve the modeling of plant-mediated transport of methane in FWMS wetlands. The bulk patch-level conductance we report is estimated at a scale equivalent with the resolution at which models define plant transport processes, and therefore, the values we report could be directly used to constrain parameterizations in similar wetlands and vegetation types. To the best of our knowledge, methane conductance through floating-leaved species has not been evaluated before, nor applied explicitly in models. Most of the parameters used in current methane models come from modeling approaches evaluated against measurements in rice

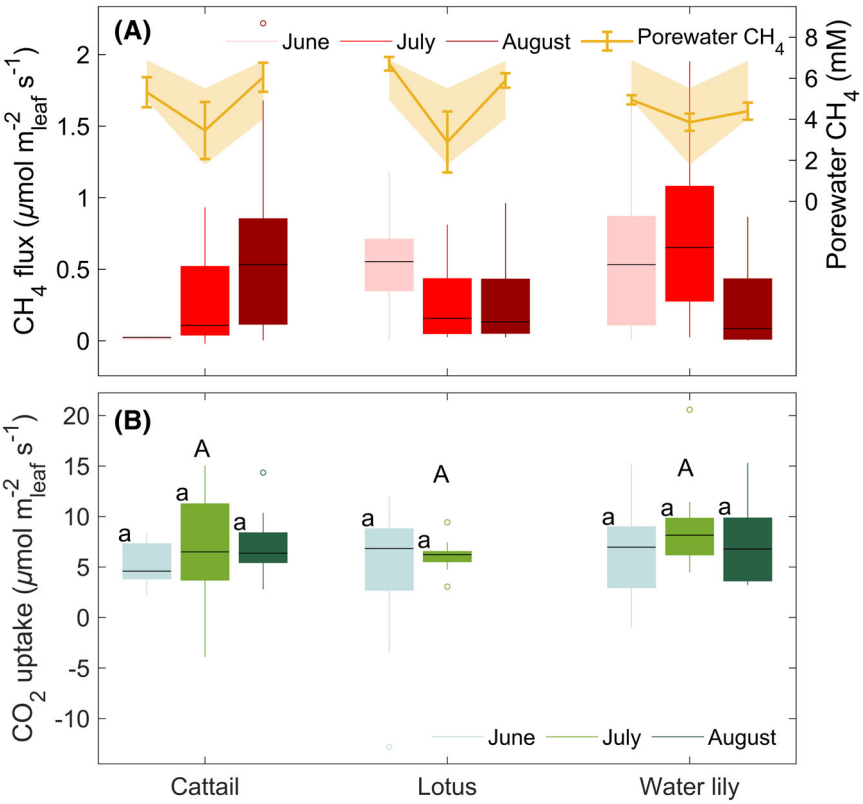

Fig. 5. Box plots of methane flux **(A)** and CO_2 uptake **(B)** for three characteristic species of FWMS wetlands sampled monthly from June through August 2018. Horizontal lines represent median values, while tops and bottoms of each box the interquartile range. Outliers, shown as circles, represent observations that are more than 1.5 times the interquartile range. Whiskers extend to the furthest observation not considered an outlier. Capital letters indicate differences at the species level while lower case letters the difference between samplings for each species. Line plots in (A) represent mean (± SEM) pore-water methane concentrations, or the vertical variability on the sediment profile (right axis). The colored bands indicate the range of low and high mean pore-water concentrations from all peepers. The values of pore-water concentrations in the cattail community correspond to a single peeper. CO_2 uptake in the lotus species in August was omitted from the analysis due to over casted stormy conditions. CO_2 uptake did not differ between species or sampling within each species.

(Sigren et al. 1997) or estimations in PFTs, such as grass, rushes, sedges, reeds, or mosses, characteristic to and observed at peatlands and not FWMS wetlands. Such values are typically derived from modeling approaches based on principles of transport and kinetics (Van Den Pol-Van Dasselaar et al. 1999; Segers and Leffelaar 2001*a*,*b*; Kettunen 2003), which to date have been applied with very limited field data (Walter and Heimann, 2000; Walter et al. 2001). Our observations suggest a lower bulk conductance of methane than previously reported for individual plants. It is important to note that the pore-water concentration of methane at our site was up to 10 times higher than the concentrations reported by other studies that measured conductance (Nouchi et al. 1994; Yavitt and Knapp, 1995), although the flux rates we observed were higher, but at a similar scale to other's observations. If the flux is not increasing linearly with pore-water concentration but increases more slowly at high concentrations (e.g., if it follows a logarithmic curve), conductances at high concentration sites will be lower than at low concentration sites. More observations of pore-water concentration, methane flux, and derived bulk conductances across many sites are needed to determine this possibility. Overall, our observations provide an important source of directly measured values of apparent bulk conductance in FWMS PFTs and indicate that parameter values used in models should not be generalized across all wetland types and PFTs.

It is easy for models to assume temporally constant parameters for conductance per leaf area and scale methane conductance per ground area following dynamic diagnosis or prescribed seasonally variable LAI. However, our results revealed significant intra-seasonal variations in methane conductance per leaf area among the three plant species (Fig. 4A). Future efforts should focus on pinning down the environmental and plant-physiological drivers of this change and developing the algorithms that allow including the seasonal dynamics of methane conductance in plant-mediated transport submodels.

As our results indicate, generalizing and including a plant-mediated transport mechanism into land-surface models based only on the correlation between methane flux and CO_2

uptake is implausible given the strong differences between species in the apparent relationship between methane and CO_2 fluxes. Including a stomatal-conductance-dependent transport mechanism into models would require detailed knowledge of the diurnal variation of methane fluxes and the role (or lack thereof) of stomata conductance in controlling methane fluxes in different species. Diurnal variation and stomata regulation of methane is currently known only in some species and unfortunately, as our results suggest, would not necessarily follow a growth-form-based PFT classification.

Nonetheless, the use of stomatal-regulated methane fluxes could represent a valuable foundation towards a more physiologically realistic representation of plant-mediated transport mechanisms for some species in future or existing mechanistic models that simulate methane biogeochemistry in spatially distributed columns and work on subdaily time steps. The spatial distribution could comprise the ecosystem scale (e.g., *ecosys*, Grant and Roulet 2002; Chang et al. 2019) or the regional scale (e.g., CLM4Me, Riley et al. 2011). With some assumptions about the shape of the daily cycle of methane conductance, it could potentially be integrated into models that work on a daily scale as well, such as wetlands DNDC (Zhang et al. 2002; Taft et al. 2019). Splitting wetlands from a single assumed "wetland" type patch to multiple patches (or sub-grid-scale tiles) of the different PFTs that compose the whole site will require a PFT-based parameterization. As we show, PFT classification that follows the growth form of wetland plants does not necessarily capture the functional type with regard to the regulation of methane fluxes. It is possible that wetland PFTs would have to be defined based on the combination of growth form and mechanisms of methane transport regulation. This may lead to an unmanageably large number of PFTs. However, given that plant zonation in most FWMS wetlands tends to be dominated by a small number of species, the parametrization can potentially be done for species with the distinction between stomata-regulated and non-stomata-regulated methane transporting species.

Besides *N. odorata* (in this study), other plant species common to FWMS wetlands, such as *Carex spp*. (Morrissey et al. 1993; Schimel 1995), *Orontium aquaticum*, *Peltandra virgnica*, *Juncus effusus*, (Garnet et al. 2005), and *Scirpus lacustris* (Van Der Nat and Middelburg 1998) show stomata-regulated methane fluxes. Species identification could be done using traditional sampling and collection, but recent developments in remote sensing techniques, coupling high-resolution multispectral imagery with machine learning are making this task less field intensive (Dronova et al. 2012; Carle et al. 2014).

Our results also suggest that incorporating methane conductance in current models based on PFT could help improve the representation of plant-mediated transport, at least for FWMS wetlands. For example, if we were to simulate methane emissions from FWMS wetlands in North America using a model such as DLEM in an approach similar to that presented by Xu & Tian (2012), choosing the median methane conductance that we found for the cattail species, instead of the median for the floating-leaved species, will lead to a twofold underestimation of plant-mediated methane transport (assuming that methane concentration in the soil is the same). Although limited in the number of species evaluated, the possible sensitivity to the plant methane conductance parameter in models warrants at the very least, the need of more measurements to probe more robustly the difference in conductance between emergent and floating leaved-species (and possibly among other PFTs) and their causes, and to understand the underlying spatial and temporal structure of the variation of conductance among regions, wetlands, seasons and species.

References

Angle, J. C., T. H. Morin, L. M. Solden, et al. 2017. Methanogenesis in oxygenated soils is a substantial fraction of wetland methane emissions. Nat. Comm. **8**: 1567. doi:10.1038/s41467-017-01753-4

Armstrong, J., and W. Armstrong. 1991. A convective throughflow of gases in *Phragmites australis* (Cav.) Trin. ex Steud. Aquat. Bot. **39**: 75–88. doi:10.1016/0304-3770(91)90023-X

Beckett, P. M., W. Armstrong, and J. Armstrong. 2001. Mathematical modelling of methane transport by *Phragmites*: The potential for diffusion within the roots and rhizosphere. Aquat. Bot. **69**: 293–312.

Beckett, P. M., W. Armstrong, S. H. F. W. Justin, and J. Armstrong. 1988. On the relative importance of convective and diffusive gas flows in plant aeration. New Phytol. **110**: 463–468. doi:10.1111/j.1469-8137.1988.tb00283.x

Bernal, B., and W. J. Mitsch. 2012. Comparing carbon sequestration in temperate freshwater wetland communities. Glob. Chang. Biol. **18**: 1636–1647. doi:10.1111/j.1365-2486.2011.02619.x

Bhullar, G. S., M. Iravani, P. J. Edwards, and H. Olde Venterink. 2013. Methane transport and emissions from soil as affected by water table and vascular plants. BMC Ecol. **13**: 32. doi:10.1186/1472-6785-13-32

Bohrer, G. 2018. AmeriFlux US-OWC Old Woman Creek. 10.17190/AMF/1418679.

Bohrer, G., Ju, Y., Arend, K., Morin, T., Rey-Sanchez, C., Wrighton, K., Villa, J. 2019. Methane and CO_2 chamber fluxes and porewater concentrations US-OWC Ameriflux wetland site, 2015–2018. AmeriFlux Management Project. 10.15485/1568865

Bridgham, S., J. Megonigal, J. Keller, N. Bliss, and C. Trettin. 2006. The carbon balance of North American wetlands. Wetlands **26**: 889–916.

Carle, M. V., L. Wang, and C. E. Sasser. 2014. Mapping freshwater marsh species distributions using WorldView-2 high-resolution multispectral satellite imagery. Int. J. Remote Sens. **35**: 4698–4716. doi:10.1080/01431161.2014.919685

Chang, K.-Y., W. J. Riley, P. M. Crill, R. F. Grant, V. I. Rich, and S. R. Saleska. 2019. Large carbon cycle sensitivities to climate across a permafrost thaw gradient in subarctic Sweden. Cryosphere **13**: 647–663. doi:10.5194/tc-13-647-2019

Chanton, J. P. 2005. The effect of gas transport on the isotope signature of methane in wetlands. Org. Geochem. **36**: 753–768. doi:10.1016/j.orggeochem.2004.10.007

Chanton, J. P., G. J. Whiting, J. D. Happell, and G. Gerard. 1993. Contrasting rates and diurnal patterns of methane emission from emergent aquatic macrophytes. Aquat. Bot. **46**: 111–128. doi:10.1016/0304-3770(93)90040-4

Chasar, L. S., J. P. Chanton, P. H. Glaser, and D. I. Siegel. 2000. Methane concentration and stable isotope distribution as evidence of rhizospheric processes: Comparison of a fen and bog in the glacial lake agassiz peatland complex. Ann. Bot. **86**: 655–663. doi:10.1006/anbo.2000.1172

Colmer, T. D. 2003. Long-distance transport of gases in plants: A perspective on internal aeration and radial oxygen loss from roots. Plant Cell Environ. **26**: 17–36. doi:10.1046/j.1365-3040.2003.00846.x

Constable, J. Y. H., J. B. Grace, and D. J. Longstreth. 1992. High carbon dioxide concentrations in aerenchyma of *Typha latifolia*. Am. J. Bot. **79**: 415–418. doi:10.1002/j.1537-2197.1992.tb14568.x

Cronk, J. K., and M. S. Fennessy. 2016. Wetland plants: Biology and ecology. CRC Press.

Dacey, J. W. H. 1980. Internal winds in water lilies: An adaptation for life in anaerobic sediments. Science **210**: 1017–1019.

Dacey, J. W. H. 1987. Knudsen-transitional flow and gas pressurization in leaves of *Nelumbo*. Plant Physiol. **85**: 199–203. doi:10.1104/pp.85.1.199

Ding, W., Z. Cai, and H. Tsuruta. 2004. Diel variation in methane emissions from the stands of *Carex lasiocarpa* and *Deyeuxia angustifolia* in a cool temperate freshwater marsh. Atmos. Environ. **38**: 181–188. doi:10.1016/j.atmosenv.2003.09.066

Ding, W., Z. Cai, H. Tsuruta, and X. Li. 2002. Effect of standing water depth on methane emissions from freshwater marshes in northeast China. Atmos. Environ. **36**: 5149–5157. doi:10.1016/S1352-2310(02)00647-7

Dronova, I., P. Gong, N. E. Clinton, L. Wang, W. Fu, S. Qi, and Y. Liu. 2012. Landscape analysis of wetland plant functional types: The effects of image segmentation scale, vegetation classes and classification methods. Remote Sens. Environ. **127**: 357–369. doi:10.1016/j.rse.2012.09.018

Elberling, B., L. Askaer, C. J. Jørgensen, H. P. Joensen, M. Kühl, R. N. Glud, and F. R. Lauritsen. 2011. Linking soil O_2, CO_2, and CH_4 concentrations in a wetland soil: Implications for CO_2 and CH_4 fluxes. Environ. Sci. Technol. **45**: 3393–3399. doi:10.1021/es103540k

Farquhar, G. D., and T. D. Sharkey. 1982. Stomatal conductance and photosynthesis. Annu. Rev. Plant Physiol. **33**: 317–345. doi:10.1146/annurev.pp.33.060182.001533

Fennessy, M. S., J. K. Cronk, and W. J. Mitsch. 1994. Macrophyte productivity and community development in created freshwater wetlands under experimental hydrological conditions. Ecol. Eng. **3**: 469–484. doi:10.1016/0925-8574(94)00013-1

Garnet, K. N., J. P. Megonigal, C. Litchfield, and G. E. Taylor. 2005. Physiological control of leaf methane emission from wetland plants. Aquat. Bot. **81**: 141–155. doi:10.1016/j.aquabot.2004.10.003

Grace, J. B., and J. S. Harrison. 1986. The biology of Canadian weeds: 73. *Typha latifolia* L., *Typha angustifolia* L. and *Typha xglauca* Godr. Can. J. Plant Sci. **66**: 361–379.

Grant, R. F., and N. T. Roulet. 2002. Methane efflux from boreal wetlands: Theory and testing of the ecosystem model Ecosys with chamber and tower flux measurements. Global Biogeochem. Cycles **16**: 1–2. doi:10.1029/2001GB001702

Grosse, W., H. Bernhard Büchel, and H. Tiebel. 1991. Pressurized ventilation in wetland plants. Aquat. Bot. **39**: 89–98. doi:10.1016/0304-3770(91)90024-Y

Henneberg, A., B. K. Sorrell, and H. Brix. 2012. Internal methane transport through *Juncus effusus*: Experimental manipulation of morphological barriers to test above-and below-ground diffusion limitation. New Phytol. **196**: 799–806.

Herdendorf, C. E., D. M. Klarer, and R. C. Herdendorf. 2006. The ecology of Old Woman Creek, Ohio: An estuarine and watershed profile, 2nd ed. Ohio Department of Natural Resources.

Hutchinson, G., and A. Mosier. 1981. Improved soil cover method for field measurement of nitrous oxide fluxes 1. Soil Sci. Soc. Am. J. **45**: 311–316.

Jeffrey, L. C., D. T. Maher, S. G. Johnston, B. P. Kelaher, A. Steven, and D. R. Tait. 2019. Wetland methane emissions dominated by plant-mediated fluxes: Contrasting emissions pathways and seasons within a shallow freshwater subtropical wetland. Limnol. Oceanogr. **64**: 1895–1912.

Joabsson, A., and T. R. Christensen. 2001. Methane emissions from wetlands and their relationship with vascular plants: An Arctic example. Glob. Change Biol. **7**: 919–932. doi:10.1046/j.1354-1013.2001.00044.x

Kampbell, D. H., J. T. Wilson, and S. A. Vandegrift. 1989. Dissolved oxygen and methane in water by a GC headspace equilibration technique. Int. J. Environ. Anal. Chem. **36**: 249–257. doi:10.1080/03067318908026878

Kankaala, P., T. Käki, S. Mäkelä, A. Ojala, H. Pajunen, and L. Arvola. 2005. Methane efflux in relation to plant biomass and sediment characteristics in stands of three common emergent macrophytes in boreal mesoeutrophic lakes. Glob. Change Biol. **11**: 145–153. doi:10.1111/j.1365-2486.2004.00888.x

Kao-Kniffin, J., D. S. Freyre, and T. C. Balser. 2010. Methane dynamics across wetland plant species. Aquat. Bot. **93**: 107–113. doi:10.1016/j.aquabot.2010.03.009

Kettunen, A. 2003. Connecting methane fluxes to vegetation cover and water table fluctuations at microsite level: A modeling study. Global Biogeochemical Cycles **17**: 1051. doi:10.1029/2002GB001958

Knapp, A. K., and J. B. Yavitt. 1992. Evaluation of a closed-chamber method for estimating methane emissions from aquatic plants. Tellus B **44**: 63–71. doi:10.3402/tellusb.v44i1.15425

Knapp, A. K., and J. B. Yavitt. 1995. Gas exchange characteristics of *Typha latifolia* L. from nine sites across North America. Aquat. Bot. **49**: 203–215. doi:10.1016/0304-3770(94)00433-M

Koebsch, F., G. Jurasinski, M. Koch, J. Hofmann, and S. Glatzel. 2015. Controls for multi-scale temporal variation in ecosystem methane exchange during the growing season of a permanently inundated fen. Agric. For. Meteorol. **204**: 94–105. doi:10.1016/j.agrformet.2015.02.002

Kolka, R., C. Trettin, K. Krauss, and others. 2018. Chapter 13: Terrestrial wetlands, p. 507–567. *In* Second state of the carbon cycle report (SOCCR2): A sustained assessment report. U.S. Global Change Research Program.

Kutzbach, L., J. Scneider, T. Sachs, and others. 2007. CO_2 flux determination by closed-chamber methods can be seriously biased by inappropriate application of linear regression. Biogeosciences **4**: 1005–1025.

Laanbroek, H. J. 2010. Methane emission from natural wetlands: Interplay between emergent macrophytes and soil microbial processes. A mini-review. Ann. Bot. **105**: 141–153. doi:10.1093/aob/mcp201

Labate, C. A., and R. C. Leegood. 1988. Limitation of photosynthesis by changes in temperature. Planta **173**: 519–527. doi:10.1007/BF00958965

Li, S., J. Lissner, I. A. Mendelssohn, H. Brix, B. Lorenzen, K. L. McKee, and S. Miao. 2010. Nutrient and growth responses of cattail (*Typha domingensis*) to redox intensity and phosphate availability. Ann. Bot. **105**: 175–184. doi:10.1093/aob/mcp213

Lorenzen, B., H. Brix, I. A. Mendelssohn, K. L. McKee, and S. L. Miao. 2001. Growth, biomass allocation and nutrient use efficiency in *Cladium jamaicense* and *Typha domingensis* as affected by phosphorus and oxygen availability. Aquat. Bot. **70**: 117–133. doi:10.1016/S0304-3770(01)00155-3

MacDonald, L. H., J. S. Paull, and P. R. Jaffé. 2013. Enhanced semipermanent dialysis samplers for long-term environmental monitoring in saturated sediments. Environ. Monit. Assess. **185**: 3613–3624. doi:10.1007/s10661-012-2813-8

Matthews, P. G. D., and R. S. Seymour. 2014. Stomata actively regulate internal aeration of the sacred lotus *Nelumbo nucifera*. Plant Cell Environ. **37**: 402–413. doi:10.1111/pce.12163

McNaughton, S. J. 1966. Ecotype function in the *Typha* community-type. Ecol. Monogr. **36**: 297–325. doi:10.2307/1942372

Mevi-Schutz, J., and W. Grosse. 1988. A two-way gas transport system in *Nelumbo nucifera*. Plant Cell Environ. **11**: 27–34.

Mitsch, W. J., J. G. Gosselink, C. J. Anderson, and L. Zhang. 2009. Wetland ecosystems. John Wiley & Sons.

Morrissey, L. A., D. B. Zobel, and G. P. Livingston. 1993. Significance of stomatal control on methane release from *Carex*-dominated wetlands. Chemosphere **26**: 339–355. doi:10.1016/0045-6535(93)90430-D

Natural Resources Conservation Service, U.S. Department Of Agriculture. 2017. Web soil survey.

Nisbet, R. E. R., R. Fisher, R. H. Nimmo, and others. 2009. Emission of methane from plants. Proc. R. Soc. B **276**: 1347–1354.

Nouchi, I., S. Mariko, and K. Aoki. 1990. Mechanism of methane transport from the rhizosphere to the atmosphere through rice plants. Plant Physiol. **94**: 59–66. doi:10.1104/pp.94.1.59

Nouchi, I., T. Hosono, K. Aoki, and K. Minami. 1994. Seasonal variation in methane flux from rice paddies associated with methane concentration in soil water, rice biomass and temperature, and its modelling. Plant and Soil **161**: 195–208. doi:10.1007/BF00046390

Pedersen, A. R., S. O. Petersen, and K. Schelde. 2010. A comprehensive approach to soil-atmosphere trace-gas flux estimation with static chambers. Eur. J. Soil Sci. **61**: 888–902. doi:10.1111/j.1365-2389.2010.01291.x

Rey-Sanchez, A. C., T. H. Morin, K. C. Stefanik, K. Wrighton, and G. Bohrer. 2018. Determining total emissions and environmental drivers of methane flux in a Lake Erie estuarine marsh. Ecol. Eng. **114**: 7–15. doi:10.1016/j.ecoleng.2017.06.042

Rey-Sanchez, C., G. Bohrer, J. Slater, Y.-F. Li, R. Grau-Andrés, Y. Hao, V. I. Rich, and G. M. Davies. 2019. The ratio of methanogens to methanotrophs and water-level dynamics drive methane transfer velocity in a temperate kettle-hole peat bog. Biogeosciences **16**: 3207–3231. doi:10.5194/bg-16-3207-2019

Richards, J. H., T. G. Troxler, D. W. Lee, and M. S. Zimmerman. 2011. Experimental determination of effects of water depth on *Nymphaea odorata* growth, morphology and biomass allocation. Aquat. Bot. **95**: 9–16. doi:10.1016/j.aquabot.2011.03.002

Riley, W., Z. Subin, D. Lawrence, S. Swenson, M. Torn, L. Meng, N. Mahowald, and P. Hess. 2011. Barriers to predicting changes in global terrestrial methane fluxes: Analyses using CLM4Me, a methane biogeochemistry model integrated in CESM. Biogeosciences **8**: 1925–1953.

Ringeval, B., N. de Noblet-Ducoudré, P. Ciais, P. Bousquet, C. Prigent, F. Papa, and W. B. Rossow. 2010. An attempt to quantify the impact of changes in wetland extent on methane emissions on the seasonal and interannual time scales. Global Biogeochem. Cycles **24**: GB2003. doi:10.1029/2008GB003354

Ritchie, R. J. 2012. Photosynthesis in the blue water lily (*Nymphaea caerulea* Saligny) using pulse amplitude modulation fluorometry. Int. J. Plant Sci. **173**: 124–136. doi:10.1086/663168

Schimel, J. P. 1995. Plant transport and methane production as controls on methane flux from arctic wet meadow tundra. Biogeochemistry **28**: 183–200. doi:10.1007/BF02186458

Schneider, E. L., and T. Chaney. 1981. The floral biology of *Nymphaea odorata* (*Nymphaeaceae*). Southwest. Nat. **26**: 159–165. doi:10.2307/3671112

Schütz, H., W. Seiler, and R. Conrad. 1989. Processes involved in formation and emission of methane in rice paddies. Biogeochemistry **7**: 33–53. doi:10.1007/BF00000896

Sebacher, D. I., R. C. Harriss, and K. B. Bartlett. 1983. Methane flux across the air-water interface: Air velocity effects. Tellus B **35B**: 103–109. doi:10.1111/j.1600-0889.1983.tb00014.x

Sebacher, D. I., R. C. Harriss, and K. B. Bartlett. 1985. Methane emissions to the atmosphere through aquatic plants. J. Environ. Qual. **14**: 40–46.

Segers, R. 1998. Methane production and methane consumption: A review of processes underlying wetland methane fluxes. Biogeochemistry **41**: 23–51. doi:10.1023/A:1005929032764

Segers, R., and P. A. Leffelaar. 2001*a*. Modeling methane fluxes in wetlands with gas-transporting plants: 1. Single-root scale. J. Geophys. Res.: Atmos. **106**: 3511–3528.

Segers, R., and P. A. Leffelaar. 2001*b*. Modeling methane fluxes in wetlands with gas-transporting plants: 3. Plot scale. J. Geophys. Res.: Atmos **106**: 3541–3558. doi:10.1029/2000JD900482

Shannon, R. D., J. R. White, J. E. Lawson, and B. S. Gilmour. 1996. Methane efflux from emergent vegetation in peatlands. J. Ecol. **84**: 239–246.

Sigren, L., G. Byrd, F. Fisher, and R. Sass. 1997. Comparison of soil acetate concentrations and methane producton, transport, and emission in two rice cultivars. Global Biogeochem. Cycles **11**: 1–14.

Smirnoff, N., and R. M. M. Crawford. 1983. Variation in the structure and response to flooding of root aerenchyma in some wetland plants. Ann. Bot. **51**: 237–249. doi:10.1093/oxfordjournals.aob.a086462

Sorrell, B. K., and P. I. Boon. 1994. Convective gas flow in *Eleocharis sphacelata* R. Br.: Methane transport and release from wetlands. Aquat. Bot. **47**: 197–212. doi:10.1016/0304-3770(94)90053-1

Taft, H. E., P. A. Cross, A. Hastings, J. Yeluripati, and D. L. Jones. 2019. Estimating greenhouse gases emissions from horticultural peat soils using a DNDC modelling approach. J. Environ. Manage. **233**: 681–694. doi:10.1016/j.jenvman.2018.11.113

Thomas, K. L., J. Benstead, K. L. Davies, and D. Lloyd. 1996. Role of wetland plants in the diurnal control of CH_4 and CO_2 fluxes in peat. Soil Biol. Biochem. **28**: 17–23. doi:10.1016/0038-0717(95)00103-4

Tian, H., C. Lu, P. Ciais, and others. 2016. The terrestrial biosphere as a net source of greenhouse gases to the atmosphere. Nature **531**: 225–228.

Tian, H., X. Xu, M. Liu, W. Ren, C. Zhang, G. Chen, and C. Lu. 2010. Spatial and temporal patterns of CH_4 and N_2O fluxes in terrestrial ecosystems of North America during 1979–2008: Application of a global biogeochemistry model. Biogeosciences **7**: 2673–2694.

Tornberg, T., M. Bendix, and H. Brix. 1994. Internal gas transport in *Typha latifolia* L. and *Typha angustifolia* L. 2. Convective throughflow pathways and ecological significance. Aquat. Bot. **49**: 91–105.

Tulbure, M. G., C. A. Johnston, and D. L. Auger. 2007. Rapid invasion of a Great Lakes coastal wetland by non-native *Phragmites australis* and *Typha*. J. Great Lakes Res. **33**: 269–279. doi:10.3394/0380-1330(2007)33[269:RIOAGL]2.0.CO;2, sp3

Van Den Pol-Van Dasselaar, A., M. L. Van Beusichem, and O. Oenema. 1999. Determinants of spatial variability of methane emissions from wet grasslands on peat soil. Biogeochemistry **44**: 221–237.

Van Der Nat, F.-J. W. A., and J. J. Middelburg. 1998. Effects of two common macrophytes on methane dynamics in freshwater sediments. Biogeochemistry **43**: 79–104. doi:10.1023/A:1006076527187

Walter, B. P., and M. Heimann. 2000. A process-based, climate-sensitive model to derive methane emissions from natural wetlands: Application to five wetland sites, sensitivity to model parameters, and climate. Global Biogeochem. Cycles **14**: 745–765. doi:10.1029/1999GB001204

Walter, B. P., M. Heimann, and E. Matthews. 2001. Modeling modern methane emissions from natural wetlands 1. Model description and results. J. Geophys. Res. **106**: 34189–34206. doi:10.1029/2001JD900165, D24

Wang, W., C. Zeng, J. Sardans, C. Wang, C. Tong, and J. Peñuelas. 2018. Soil methane production, anaerobic and aerobic oxidation in porewater of wetland soils of the Minjiang River Estuarine, China. Wetlands **38**: 627–640. doi:10.1007/s13157-018-1006-9

Weisner, S. E. B. 1993. Long-term competitive displacement of *Typha latifolia* by *Typha angustifolia* in a eutrophic lake. Oecologia **94**: 451–456.

White, S. D., and G. G. Ganf. 2000. Influence of stomatal conductance on the efficiency of internal pressurisation in *Typha domingensis*. Aquat. Bot. **67**: 1–11. doi:10.1016/S0304-3770(99)00090-X

Whiting, G. J., and J. P. Chanton. 1996. Control of the diurnal pattern of methane emission from emergent aquatic macrophytes by gas transport mechanisms. Aquat. Bot. **54**: 237–253.

Whyte, R. S., D. A. Francko, and D. M. Klarer. 1997. Distribution of the floating-leaf macrophyte *Nelumbo lutea* (American water lotus) in a coastal wetland on Lake Erie. Wetlands **17**: 567–573. doi:10.1007/BF03161523

Xu, X., D. A. Elias, D. E. Graham, T. J. Phelps, S. L. Carroll, S. D. Wullschleger, and P. E. Thornton. 2015. A microbial functional group-based module for simulating methane production and consumption: Application to an incubated permafrost soil. Biogeosciences **120**: 1315–1333. doi:10.1002/2015JG002935

Xu, X., and H. Tian. 2012. Methane exchange between marshland and the atmosphere over China during 1949–2008. Global Biogeochemical Cycles **26**: GB2006. doi:10.1029/2010GB003946

Xu, X., F. Yuan, P. J. Hanson, and others. 2016. Reviews and syntheses: Four decades of modeling methane cycling in terrestrial ecosystems. Biogeosciences **13**: 3735–3755.

Yavitt, J. B., and A. K. Knapp. 1995. Methane emission to the atmosphere through emergent cattail (*Typha latifolia* L.) plants. Tellus B **47**: 521–534. doi:10.3402/tellusb.v47i5.16065

Yavitt, J. B., and A. K. Knapp. 1998. Aspects of methane flow from sediment through emergent cattail (*Typha latifolia*) plants. New Phytol. **139**: 495–503.

Zhang, Y., C. Li, C. C. Trettin, H. Li, and G. Sun. 2002. An integrated model of soil, hydrology, and vegetation for carbon dynamics in wetland ecosystems. Global Biogeochem. Cycles **16**: 1061.

Zhu, Q., J. Liu, C. Peng, and others. 2014. Modelling methane emissions from natural wetlands by development and application of the TRIPLEX-GHG model. Geosci. Model Dev. **7**: 981–999.

Acknowledgments

This study was supported by the Ohio Water Development Authority (award 7880), Ohio Water Resources Research Center (award G16AP00076), NOAA Davidson Fellowship and Student Development opportunities Grant through ODNR Grant Agreement N18B315-11, and based partially upon work supported by an Early Career Award to Kelly Wrighton from the U.S. Department of energy, Office of Science, Office of Biological and Environmental Research (award DE-SC0018022). Taylor Stephen participation in this project was sponsored by the Summer Research Opportunities Program (SROP). Site access, meteorology and water observations, and technical support were provided by Kristin Arend (NERR/NOAA/ODNR). Data of chamber fluxes and pore-water concentration measurements for the site, including those used in this manuscript, are available through ESS-DiVE (https://data.ess-dive.lbl.gov/view/doi:10.15485/1568865). Fluxes and meteorological data for the OWC site is available through the Ameriflux database, site ID: US-OWC. Funding for processing EC flux data was provided by the U.S. Department of Energy's Office of Science through the Ameriflux project.

Conflict of interest

The authors declared no potential conflict of interests.

Submitted 30 October 2019
Revised 03 March 2020
Accepted 29 April 2020

Associate editor: Ryan Sponseller